



Originally published as:

Nowaczyk, N., Worm, H.-U., Knecht, A., Hinken, J. H. (1998): Imaging distribution patterns of magnetic minerals by a novel high-Tc-SQUID-based field distribution measuring system: application to Permian sediments. - *Geophysical Journal International*, 132, 3, pp. 721—724.

DOI: <https://doi.org/10.1046/j.1365-246X.1998.00496.x>

RESEARCH NOTE

# Imaging distribution patterns of magnetic minerals by a novel high- $T_c$ -SQUID-based field distribution measuring system: application to Permian sediments

Norbert R. Nowaczyk,<sup>1</sup> Horst-Ulrich Worm,<sup>2</sup> Andrea Knecht<sup>3</sup>  
and Johann H. Hinken<sup>3</sup>

<sup>1</sup> *GeoForschungsZentrum Potsdam, Projektbereich 3.3, Laboratory for Palaeo- and Rock Magnetism, Telegrafenberg, D-14473 Potsdam, Germany. E-mail: nowa@gfz-potsdam.de*

<sup>2</sup> *Institut für Geophysik, Universität Göttingen, Herzberger Landstr. 180, 37075 Göttingen, Germany*

<sup>3</sup> *F.I.T. Messtechnik GmbH, Postfach 1147, D-31158 Bad Salzdetfurth, Germany*

Accepted 1997 November 5. Received in original form 1997 June 23

## SUMMARY

A newly developed field distribution measuring system based on a high- $T_c$  SQUID has been employed in the study of magnetic mineral distribution in several Permian sedimentary rocks. The instrument consists of a small,  $1.4 \times 1.4$  mm sized YBaCu-oxide SQUID magnetic field sensor that is operated in a thin-walled dewar, so that the sample's surface, at room temperature, can be scanned at a distance of only  $\sim 1.5$  mm. The samples were subjected to a saturation remanence perpendicular to the surface and the scanning measurements in zero field reveal that the magnetization might be carried by only a small part of a sample, in one case associated with secondary oxide phases. High-resolution magnetic scans can aid in the interpretation of the magnetic remanence acquisition process.

**Key words:** high-temperature SQUID, remanent magnetization.

## INTRODUCTION

The reliability of a palaeomagnetic study depends critically on the nature of the measured palaeoremanence (Van der Voo 1990), i.e. whether it was acquired synchronously with the deposition of a sediment or during a later stage. Hydrothermal activities, for example, may have led to the formation of a chemical remanent magnetization (CRM). Reheating events during burial and metamorphism produce thermoviscous overprints. Subsequent weathering can result in dissolution of the original magnetic minerals and precipitation and growth of Fe hydroxides. Depending on the mode of formation, magnetic minerals can be distributed inhomogeneously within a rock and the resulting magnetic anisotropy will in general decrease the directional fidelity of a palaeofield remanence. Microscopic methods for analysing the magnetic mineral distribution are often hampered by low concentrations (especially in sedimentary rocks), the small grain size, and problems with preparing useful thin sections. The usefulness of a magnetic scanning technique with a millimetre resolution in the study of rocks has been demonstrated once before (Thomas, Moyer & Wikswo 1992); however, the technical difficulty of operating a low- $T_c$  SQUID (superconducting quantum interference device)

at a millimetre distance from a sample at room temperature has apparently prevented routine applications. The discovery of high- $T_c$  superconductors and the ensuing development of high- $T_c$  SQUIDs that operate with liquid nitrogen facilitated applications that are hardly possible with conventional low-temperature SQUIDs. The much increased operating temperature allows the use of thin-walled dewars so that samples can be magnetically scanned from a small distance. We have employed a high- $T_c$ -SQUID-based scanning apparatus to monitor the distribution of magnetic minerals within a rock sample. The 'HFD field distribution measuring system' has been developed by F.I.T. Messtechnik GmbH, Bad Salzdetfurth, Germany, on the basis of a ceramic high- $T_c$  SQUID, for 2-D magnetic-field scans on material surfaces. To illustrate the possibilities of the system this study investigates the magnetic structure of different Permian rocks from various localities. The results yield useful information regarding the textural association of the magnetic minerals and thus on the origin of the palaeomagnetic remanence.

## METHODS AND MATERIALS

The key component of the HFD field distribution measuring system (Fig. 1) is a ceramic YBaCu-oxide SQUID sensor, only

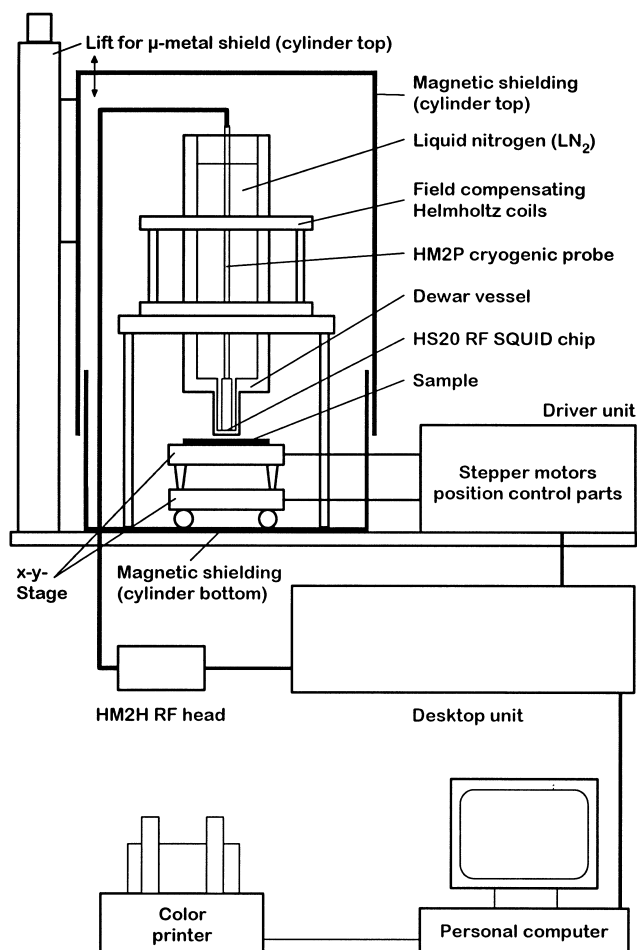


**Figure 1.** Sketch of the complete HFD field distribution measuring system for 2-D scans of the magnetic field above a test sample.

1.4 × 1.4 mm in size, allowing the same spatial resolution in the  $x$  and  $y$  directions. It is mounted at the bottom of a non-magnetic stainless steel dewar of only 1 mm wall thickness. The small dimensions allow for a high spatial field resolution. Samples with flat surfaces are attached to an  $X$ – $Y$  stage beneath the dewar. The  $X$ – $Y$  stage is moved by computer-controlled motors and can accommodate samples with a maximum size of 50 mm in the  $x$  direction and 130 mm in the  $y$  direction. The SQUID and stage are housed inside a highly efficient magnetic shielding chamber. The residual field is below 100 nT. The SQUID sensor measures the vertical component of the stray field above the test sample. Data acquisition and stage operation are fully computer-operated. The noise level of the SQUID is  $<4.5 \text{ pT Hz}^{-1/2}$  and the dynamic range is 112 dB. The horizontal resolution of about 1.5 mm implies that in order to obtain maximum resolution the samples have to be cut into thin slices. Otherwise, the far-field contributions of portions of the sample not directly adjacent to the sensor will broaden the measured anomalies and thus reduce the spatial resolution. The instrument's capabilities in detecting magnetic mineral distributions are exemplified by measurements on four different types of rock, all of middle Permian age. Sample 1 is a patchy greyish and reddish silty sandstone from the 'Oberrotliegend', Germany. The red colour is distributed irregularly within this sandstone. Sample 2 is a

finely laminated grey sandstone from the Cherry Canyon formation, Texas, USA. Sample 3 is a slightly weathered, light brownish limestone from the Bell Canyon formation, Texas, USA. Sample 4 is also from the Cherry Canyon formation, and is composed partly of a fine-grained, dark grey, homogeneous limestone and partly of a coarse-grained, laminated, light greyish to brownish limestone.

## Measurements

Slices 1 mm thick were cut from the centre of standard cylindrical palaeomagnetic samples, yielding rectangular plates with a size of 25.4 × 22 mm. For reasons of stability the slices were then glued onto 1 mm thick glass plates. Prior to slicing, the cylindrical rock samples were subjected to detailed isothermal remanent magnetization (IRM) acquisition experiments at the Laboratory for Palaeo- and Rock Magnetism, GFZ Potsdam, using a 2G Enterprises pulse magnetizer, in order to reveal the overall composition of the magnetic phase (Fig. 2). After slicing, the pulse magnetizer was used again to imprint a saturation isothermal remanent magnetization (SIRM) perpendicular to the surface of the slices, in order to produce a well-defined input signal. The field strength used for this experiment was 2.7 T. By this method the magnetic field component perpendicular to the surface is proportional to the magnetic moment of the carriers of magnetic remanence. The saturation remanence depends not only on the mineralogy but also on the grain size of the ferrimagnetic minerals. Magnetite and haematite possess very different saturation magnetizations ( $92$  versus  $0.4 \text{ A m}^2 \text{ kg}^{-1}$ ). The ratio of saturation remanence to saturation magnetization is  $M_{rs}/M_s = 0.5$  for (submicroscopic) single-domain grains and may be as low as  $M_{rs}/M_s < 0.01$  for multidomain grains larger than 50  $\mu\text{m}$  (e.g. Stacey & Banerjee 1974). The distance between the sample and the outer cryostat wall (SQUID sensor) was 1 mm (2 mm distance to the SQUID) for sample 1, because of its strong magnetization, and 0.03 mm (1 mm to the SQUID) for samples 2, 3 and 4. The samples were scanned by 0.5 mm in both the  $x$  and  $y$  directions.

## RESULTS

The results of the high-resolution 2-D scans performed across the four slices are shown in colour code in Fig. 3. The same shading, from blue, through green, yellow and red, to white was scaled to the total range of the magnetic field measured above each sample, in order to display the relative variations in magnetization. Evidently, the samples possess widely varying magnetizations. The strongest fields were measured for sample 1 (up to 2000 nT), and the weakest sample has maximum fields greater than 15 nT, still three orders of magnitude above the noise level of the instrument.

### Sample 1

The magnetization is the strongest ( $\text{SIRM} = 11.2 \text{ A m}^{-1}$ ) of all samples, yielding maximum field values of 2000 nT (Fig. 3a) with the SQUID sensor about twice as high above this sample as during scanning of the other three samples. Prominent lows in the field strength (coded as blue colours) can be related to larger areas of the greyish parts of the sandstone, and highs (red and white colours) are clearly linked to the red patches visible within the slice. Obviously, the magnetization

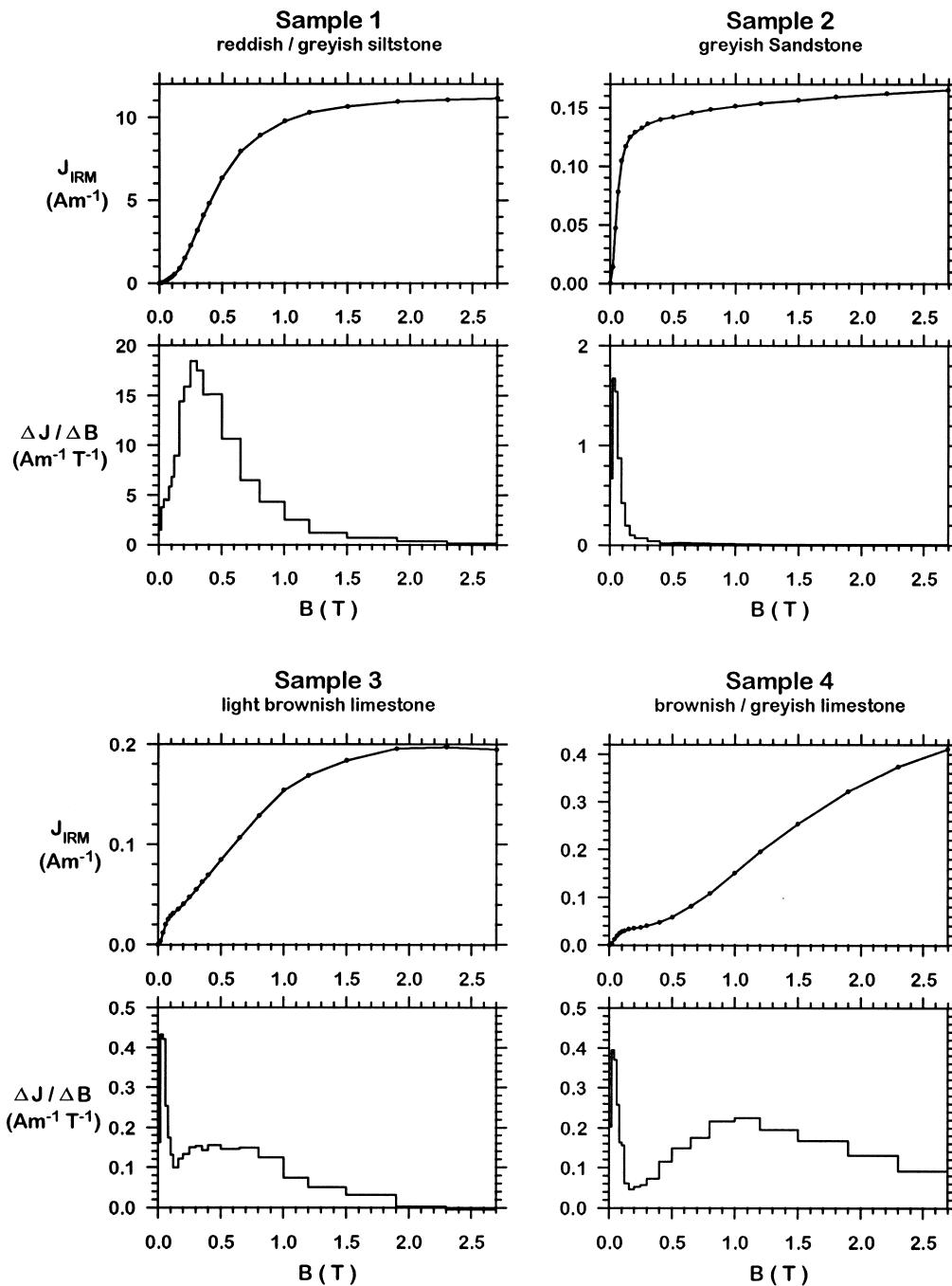


**Figure 2.** Acquisition curves of isothermal remanent magnetization (IRM) together with the acquisition rate of the four Permian sedimentary rock samples investigated.

is concentrated in the reddish parts of this sample. The IRM curve (Fig. 2) shows little acquisition below 0.2 T and thus reveals haematite as the only magnetic mineral. In this case the results of scanning really reflect the concentration variations of this high-coercivity magnetic mineral.

### Sample 2

The IRM acquisition curve (Fig. 2) of the bulk sample indicates a low concentration of (ferri-) magnetic minerals (SIRM = 0.17 A m<sup>-1</sup>). The main carrier is presumably magnetite with coercivity <0.2 T. However, a high-coercivity

mineral, haematite or goethite, is also present, which contributes about 10 per cent to the SIRM (but about 95 per cent to the bulk concentration of magnetic minerals, in the case of haematite). Magnetic scanning (Fig. 3b) indicates a rather homogeneous distribution of the magnetic minerals, with only a few spatial variations that are not linked to the orientation of the laminations visible within the slice.

### Sample 3

The IRM acquisition curve (Fig. 2) reveals that about 20 per cent of the SIRM is carried by magnetite and 80 per cent

by haematite ( $\text{SIRM} = 0.19 \text{ A m}^{-1}$ ). The distribution of the magnetization as derived from the field scan (Fig. 3c) is very inhomogeneous. About three-quarters of the slice is almost non-magnetic, indicated by the green colours. A very complex fine-scale pattern of pronounced positive and negative field values is interpreted to indicate that the magnetization is concentrated in only a small vein in the left-hand half of the slice.

#### Sample 4

The SIRM ( $0.41 \text{ A m}^{-1}$ ) is also due to a mixture of low- and high-coercivity minerals (Fig. 2). Besides about 10 per cent of the remanence being due to magnetite, the IRM acquisition curve also yields evidence for both haematite and goethite. The curve clearly does not reach saturation in a field of 2.7 T, which we take as evidence for goethite. Magnetic scanning (Fig. 3d) reveals that the magnetization is concentrated in the weathered section of the sample, which can be recognized from the brownish colours. This might indicate that the field anomaly pattern is dominated by goethite, a typical weathering product of iron-bearing minerals.

#### CONCLUSIONS

High-resolution 2-D scans across slices cut from four different rock types demonstrate that the newly developed HFD field distribution measuring system from F.I.T. is capable of revealing the distributions of magnetic carrier minerals. Magnetic scanning

aids in deciphering the nature of magnetic remanence, with a horizontal resolution of about 1.5 mm. Although this pilot study has concentrated on measuring only SIRM distribution patterns, it is certainly feasible to monitor magnetization changes after each IRM acquisition step (or during back-field curves) in order to detect spatial coercivity patterns. Finally, the HFD instrument offers the opportunity to study 3-D magnetization patterns of the (in)homogeneity of the sample if three orthogonal sections are cut from one sample. The easy-to-operate instrument and the largely automated measurements facilitate routine use in the study of magnetic texture.

#### ACKNOWLEDGMENTS

We wish to thank M. Menning (GFZ Potsdam) for providing the palaeomagnetic rock samples and M. Köhler and D. Berger (GFZ Potsdam) for preparing the thin sections. IRM measurements were performed by M. Weber (guest student from University of Cologne, Germany).

#### REFERENCES

- Stacey, F.D. & Banerjee, S.K., 1974. *The Physical Principles of Rock Magnetism*, Elsevier, Amsterdam.
- Thomas, I.M., Moyer, T.C. & Wikswo, J.P., 1992. High resolution imaging of geological thin sections: pilot study of a pyroclastic sample from the Bishop Tuff, California, USA, *Geophys. Res. Lett.*, **19**, 2139–2142.
- Van der Voo, R., 1990. The reliability of paleomagnetic data, *Tectonophysics*, **184**, 1–10.